Article:
Long, F., Hagston, W.E., Harrison, P. et al. (1997) The structural dependence of the effective mass and Luttinger parameters in semiconductor quantum wells. Journal of Applied Physics, 82 (7). pp. 3414-3421. ISSN: 1089-7550

https://doi.org/10.1063/1.365657

The structural dependence of the effective mass and Luttinger parameters in semiconductor quantum wells

Fei Long[a] and W. E. Hagston
Department of Applied Physics, University of Hull, HU6 7RX, United Kingdom

P. Harrison
Department of Electronic and Electrical Engineering, University of Leeds, LS2 9JT, United Kingdom

T. Stirner
Department of Applied Physics, University of Hull, HU6 7RX, United Kingdom

(Received 6 May 1997; accepted for publication 24 June 1997)

A detailed comparison of the empirical pseudopotential method with single and multiple band calculations based on the envelope function and effective mass approximations are presented. It is shown that, in order to give agreement with the more rigorous microscopic approach of the pseudopotential method, structural dependent effective masses and Luttinger parameters must be invoked. The CdTe/$Cd_{1-x}Mn_xTe$ system has been employed as an example, and the first pseudopotential calculations of quantum wells and superlattices in this material are presented. It is shown that the electron, light- and heavy-hole effective masses tend towards twice their bulk values in the limit of narrow quantum wells. © *1997 American Institute of Physics.*
[S0021-8979(97)00319-8]

I. INTRODUCTION

The envelope function and effective mass approximations have been employed extensively in the determination of electronic states in semiconductor heterostructures such as quantum wells and superlattices following the early work by Nedorezov[1] and Bastard.[2,3] In this approach, the periodic interatomic potential is eliminated from the description and is replaced by a smoothly varying macroscopic potential determined by the band offset of the materials. The wavefunction of the system is assumed to be a linear combination of the product of a slowly varying envelope function together with a Bloch function appropriate to a bulk carrier. The latter changes rapidly on an interatomic scale, with a period of unit cell length, and can be eliminated from the description.[4] Indeed the approach offers a simple but successful way to interpret experimental data from ''large systems'' such as wide quantum wells or long period superlattices.[5–8] It is to be noted, however, that these successes rely, to some extent, on the judicious choice of important parameters such as the effective masses of the carriers.

In contrast with the large system, the envelope function approach was shown to be less effective in describing the electronic properties of ''small systems'' such as narrow quantum wells, or short period superlattices, if one employed the same input parameters as with the large system.[9–11] Indeed, when the characteristic dimensions of the systems decrease to values comparable with the interatomic length scale, e.g., less than 20 Å, say, there exists dramatic differences between the results based on the envelope function approximation and the experimental data.[12] It is evident that some of the basic approximations used in the envelope function approach are not valid for these small systems. For example, the envelope function and the macroscopic potential change on a scale comparable with those of the Bloch function and the periodic interatomic potential, hence they can no longer be regarded as slowly varying in this case. Furthermore, the effective masses parameters (or equivalently, the Luttinger parameters), which incorporate the effect of microscopic potential change in the parametrization scheme, are normally treated as constants which are derived from band structure properties associated with the corresponding bulk materials. One can expect such a treatment to become increasingly inappropriate as the characteristic dimension of the system decreases. Although some progress has been made with regard to the general formalism of the envelope function and effective mass theory for heterostructures,[13–16] the central problems mentioned above relating to the values of the effective masses to be employed in a given calculation remain largely unresolved.

Although computationally costly, solving the Schrödinger equation with *microscopic* atomic potentials is widely employed in band structure calculations such as the semiempirical pseudopotential or the tight-binding method. The developments that have made use of these methods extend from band structure calculations of bulk materials to those of microstructures.[17,18,20] In particular, Jaros *et al.*[18,19] and Zunger *et al.*[20–24] have developed two different schemes for pseudopotential calculations of semiconductor heterostructures, which can handle efficiently both small and large systems. These pseudopotential calculations are, of course, free from the approximations and restraints to which the envelope function approach suffers. Consequently, a comparison of the predictions of both methods permits a direct evaluation of the limitation of the envelope function approach and the modifications to it that are needed in order to give agreement with the exact results of the pseudopotential theory.

In the present article, which is an extension of our recent work on the band structure and effective masses of the bulk $Cd_{1-x}Mn_xTe$ alloy,[25] we perform the first empirical pseudo-

[a]Electronic mail: f.long@apphys.hull.ac.uk

 0021-8979/97/82(7)/3414/8/$10.00

potential calculations of (001)CdTe/$Cd_{1-x}Mn_xTe$ superlattices and quantum wells. These results are then compared with those from a simple single band model and with a multiband $\mathbf{k}\cdot\mathbf{p}$ model, both of which encompass the envelope function and effective mass approximations. In particular, the effective masses of the electron, light- and heavy-holes in the quantum wells have been determined by treating them as parameters within the envelope function calculation and adjusting them until the resultant energy level structure agrees with that of the empirical pseudopotential method. In this manner, we can deduce, for the first time, the dependencies of the effective masses of the electron, light- and heavy-holes in (001) $Cd_{1-x}Mn_xTe$/CdTe superlattices and quantum wells, on the width of the wells, a feature which has received scant attention to date.

II. PSEUDOPOTENTIAL CALCULATION OF THE SUPERLATTICES AND QUANTUM WELLS

In this section, we describe the empirical pseudopotential calculation for the diluted magnetic semiconductor (DMS) $Cd_{1-x}Mn_xTe$/CdTe superlattices grown along the (001) direction. There are extensive experimental[10,26,27] and theoretical[8,28–30] studies of these DMS quantum well systems. These have led to a great understanding of their novel properties due to the large sp^3-d exchange interaction between the carriers and the magnetic Mn^{2+} ions. However, the majority of these studies have been based on the envelope function and effective mass approximations.

The calculational scheme used here was first developed by Jaros *et al.*[18,19,31,32] who applied it to evaluate the electronic structure of types I and II superlattices of III–V and II–VI compound semiconductors. In the calculation, a superlattice unit cell is chosen so that the length of the superlattice period lies along the growth direction. The Schrödinger equation for the superlattice is written as

$$(\mathscr{H}_0+V)\Psi=E\Psi, \tag{1}$$

where $\mathscr{H}_0$ is the Hamiltonian of the bulk zinc-blende CdTe crystal while V is the perturbation introduced to account for the difference in the microscopic atomic potential between CdTe and $Cd_{1-x}Mn_xTe$. This occurs, within the unit cell, when the latter substitute the former thus creating the superlattice. The superlattice wavefunction is constructed as a linear combination of the eigenfunctions of $\mathscr{H}_0$, i.e.,

$$\Psi(\mathbf{r})=\sum_{n,\mathbf{k},S} a_{n,\mathbf{k},s}\Phi_{n,\mathbf{k},s}(\mathbf{r}), \tag{2}$$

where n and s are, respectively, the band and spin index of the bulk CdTe system. The wave vector $\mathbf{k}$ lies in the bulk Brillouin zone and is determined by the period of the perturbation V. This is because the bulk states $\Phi_{n,\mathbf{k}}(z)$ which contribute significantly to the superlattice state $\Psi_{k_s}(z)$ having the superlattice wave vector $\mathbf{k}_s$, are those having a $\mathbf{k}$ vector which can couple to $\mathbf{k}$ by some linear combination of the superlattice reciprocal lattice vectors. It is only those bulk states which satisfy this condition that need to be included in the expansion of the superlattice state in Eq. (2). In the present work, only the $\bar{\Gamma}$ point in the superlattice Brillouin zone is considered since the quantum wells and superlattices discussed in this work are type I. Consequently, the only wave-vector $\mathbf{k}_s$ which needed to be included in Eq. (2) are the set

$$\frac{2\pi}{a_0}\left(0,0,\frac{m}{N}\right), \tag{3}$$

where a_0 is the lattice constant of bulk CdTe, i.e., 6.481 Å. The entity N is the number of lattice constants in a superlattice unit cell and the m are the integers satisfying $m\leqslant N$. $\Phi_{n,k,s}$ is generated by the standard local pseudopotential calculation including spin-orbit coupling,[11,25,33] i.e., by directly diagonalizing the matrix equation

$$\left|\left[\frac{1}{2}k^2-E_{n\mathbf{k}s}\right]\delta_{\mathbf{G},\mathbf{G}'}\delta_{s,s'}+V_L(|\mathbf{G}-\mathbf{G}'|)\delta_{s,s'}+V^{s-o}_{s,s'}(\mathbf{K},\mathbf{K}')\right|=0, \tag{4}$$

where $\mathbf{G}$ is a bulk reciprocal lattice vector, and $\mathbf{K}=\mathbf{k}+\mathbf{G}$. $E_{n\mathbf{k}s}$ is the eigenvalue corresponding to $\Phi_{n\mathbf{k}s}$. $V^{s-o}_{s,s'}$ is the spin-orbit coupling matrix element which is evaluated using the method introduced by Bloom and Bergstresser.[34] V_L is the screened local atomic pseudopotential. Knowledge of the appropriate value of V_L for CdTe, MnTe, and $Cd_{1-x}Mn_xTe$ is essential to this work. V_L for CdTe and MnTe are determined by adjusting the form factors V(G), i.e., the Fourier transformed components of V_L, in order that the resulting band structures and effective masses of the bulk materials agree with those from experimental data.

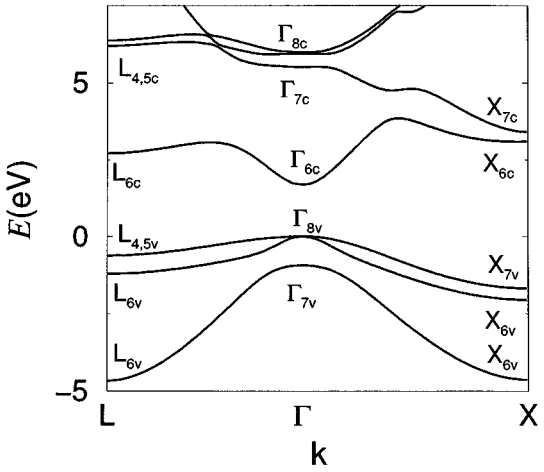

FIG. 1. The band structure of the bulk $Cd_{0.9}Mn_{0.1}Te$ obtained from the pseudopotential calculation.

Figure 1 is a typical band structure for the $Cd_{1-x}Mn_xTe$ alloy with $x = 0.1$. This alloy will be used as the barrier material in later calculations. It is worth pointing out that although the 3d electron energy bands do not appear explicitly in Fig. 1, their effects on the electrons in the conduction and valence bands have been included implicitly in the calculations, further details of which can be found in our recent work.[25]

TABLE I. Comparison of the critical point energies of bulk CdTe as obtained in the present pseudopotential calculation with those obtained in the nonlocal pseudopotential by Chelikowsky and Cohen[a] (CC). The eigenvalues for bulk MnTe are also listed and the way to compare them to *ab initio* calculation is detailed in our recent work. [b]

	CdTe		
Energy level (eV)	Present	CC	MnTe
Γ_{7v}	−0.920	−0.89	−0.922
Γ_{8v}	0.000	0.00	0.000
Γ_{6c}	1.606	1.59	3.193
Γ_{7c}	5.384	5.36	6.837
X_{6v}	−4.799	−5.05	−4.306
X_{7v}	−2.011	−1.98	−2.025
X_{6v}	−1.700	−1.60	−1.568
X_{6c}	3.097	3.48	3.814
L_{6v}	−4.686	−4.73	2.812
L_{6v}	−1.212	−1.18	−1.357
$L_{4,5}$	−0.646	−0.65	−0.873
L_{6c}	2.831	2.82	4.795
L_{6c}	6.127	6.18	5.797

[a]See Ref. 45.
[b]See Ref. 25.

TABLE II. Comparison of the other band properties of bulk CdTe and MnTe calculated by the pseudopotential approach employed in the present work with the experiments. These properties are also used as the input parameters for the single- and multiple-band effective mass model calculations in the present work.

	CdTe		MnTe	
Property	Present	Experiment	Present	Experiment
$E_{\text{gap}}^{\text{dir}}$ (eV)	1.606	1.606[a]	3.193	3.193 [d]
Δ_0 (eV)	0.920	0.92 [b]	0.922	
Effective masses				
at Γ point (m_0)				
m_e[100]	0.110	0.099[a]	0.177	
m_{hh}[100]	0.60	0.60[c]	0.961	
m_{lh}[100]	0.18	0.12[c]	0.322	
m_{so}[100]	0.35		0.530	
m_{hh}[111]	0.69	0.69[c]	1.01	
m_{lh}[111]	0.21	0.11[c]	0.37	
Luttinger parameters				
γ_1	3.611 111		2.073 086	
γ_2	0.972 222		0.516 252	
γ_3	1.080 918		0.541 494	
α	8.212 3137		4.724 169	
E_p (eV)	9.973 908		8.004 573	

[a]Ref. 46.
[b]Ref. 47.
[c]Ref. 44.
[d]Ref. 48.

The relative alignment between CdTe and $Cd_{1-x}Mn_xTe$ is determined by the symmetric part $V_L^S(G)$ of V(G) associated with MnTe at $G=0$. In effect, $V_L^S(G)$ causes a rigid shift of the whole band structure, and its value was adjusted so that 35% of the difference in the band gap between CdTe and MnTe at the Γ point was taken up by the valence-band offset. Although the exact values of the valence-band offset between CdTe and $Cd_{1-x}Mn_xTe$ are still controversial,[26,35] recent experimental work[36] suggests that the values are within the range of 30%–40%.

It is known that the form factors $V(q)$ for small $\mathbf{q}$, in addition to those for the bulk zinc blende reciprocal lattice vectors, are needed in an empirical pseudopotential calculation of superlattices. Several attempts[19,37,38] at determining these small $\mathbf{q}$ form factors, based essentially on the quasicontinuous dependencies of $V(q)$ on q, have been made. These have involved fitting a parameterized algebraic form of potential $V(q)$, to the form factors at the zinc-blende reciprocal lattice vectors. The parameters are then optimized in order that a variety of bulk properties, such as the band structure, effective masses, band offsets, and deformation potentials agree with the measured values. In the present work, the quasicontinuous forms of $V(q)$ for CdTe and MnTe are assumed to be a polynomial of degree 8, i.e.,

$$V(q)=\sum_{i=0}^{8} A_i q^i. \tag{5}$$

The polynomial is first fitted to $V(G)$ at the zinc-blende vectors, which means that the measured band structure and effective masses of bulk materials have been reproduced. Then, for CdTe, the gradients of the polynomial at the different zinc-blende reciprocal vectors $\mathbf{G}$ are optimized so that a variety of measured deformation potentials[39] are reproduced by the pseudopotential calculation. For MnTe and $Cd_{1-x}Mn_xTe$, because of the scant knowledge available concerning the deformation potentials, we first made a ''best guess'' at the gradients of the polynomial. This polynomial form of $V(q)$ is then used in a calculation of a large period superlattice. For the latter, it has been shown in the literature, e.g., Ref. 9, that calculations based on microscopic potential models, such as the pseudopotential or tight-binding approaches, give good agreement with those from the simple envelope function approach within the effective mass approximation. Consequently we adjusted the gradients of the polynomial at the zinc- blende vectors so that the calculated energy levels of a given large period superlattice, (e.g., 207.4 Å $Cd_{1-x}Mn_xTe$/90.7 Å CdTe) agree with those of the simple envelope function approach. The critical point energies of bulk CdTe and MnTe calculated by the pseudopotential approach employed in the present work are shown in Table I. Similarly Table II shows the other band properties of bulk CdTe and MnTe calculated which are also used as the input parameters for the single- and multiple-band effective mass model calculation performed in the present work. Table III lists the coefficients of the polynomial functions of V(q) for CdTe and MnTe.

Using the quasicontinuous form of $V(q)$ for CdTe and $Cd_{1-x}Mn_xTe$, the energy levels of the superlattices and quantum wells are obtained by substituting Eq. (2) into Eq. (1) and directly diagonalizing the resulting matrix equation.

III. ENVELOPE-FUNCTION TECHNIQUE

In this section, we describe the calculations based on the envelope function approximation and compare them with the results obtained from the empirical pseudopotential approach. Two classes of model were employed within the envelope function approach

TABLE III. Coefficients of the polynomial function of atomic pseudopotential form factors $V(q)$. The unit of $V(q)$ is eV and that of $\mathbf{q}$ is $2\pi/a_0$.

Coefficients	Cd	Te (in CdTe)	Mn	Te (in MnTe)
A_0	$7.246\,454\times10^{-3}$	$2.145\,514\times10^{-2}$	$-1.251\,439\times10^{-2}$	$-2.275\,829\times10^{-3}$
A_1	$-2.969\,039\times10^{-2}$	$-2.403\,953\times10^{-1}$	$-1.346\,197\times10^{-1}$	$-1.346\,197\times10^{-1}$
A_2	$3.081\,176\times10^{-2}$	$1.201\,461\times10^{-1}$	$2.089\,711\times10^{-1}$	$-2.956\,334\times10^{-2}$
A_3	$-2.110\,671\times10^{-2}$	$-3.258\,573\times10^{-2}$	$-2.411\,621\times10^{-2}$	$-4.366\,798\times10^{-2}$
A_4	$5.797\,186\times10^{-3}$	$5.442\,722\times10^{-3}$	$6.123\,684\times10^{-3}$	$8.046\,649\times10^{-3}$
A_5	$-7.518\,004\times10^{-4}$	$-5.430\,282\times10^{-4}$	$-7.514\,777\times10^{-4}$	$-8.601\,845\times10^{-4}$
A_6	$4.993\,662\times10^{-5}$	$3.101\,786\times10^{-5}$	$4.802\,937\times10^{-5}$	$5.155\,391\times10^{-5}$
A_7	$-1.649\,341\times10^{-6}$	$-9.314\,154\times10^{-7}$	$-1.542\,507\times10^{-6}$	$-1.602\,978\times10^{-6}$
A_8	$2.150\,615\times10^{-8}$	$1.138\,057\times10^{-8}$	$1.968\,992\times10^{-8}$	$2.011\,061\times10^{-8}$

(1) the single-band effective mass model—although the couplings between electrons in different bands are not included explicitly in this kind of model, it still gives a good description of band-edge states of a large quantum well system provided an appropriate choice of the effective masses is made.
(2) the multiband $\mathbf{k}\cdot\mathbf{p}$ model—a perturbation theory in which a small set of coupled zone-center states of the different bands are used to give a description of the band structures and other related electronic properties of bulk materials and corresponding heterostructures.

In the class (i) model, the Schrödinger equation of a quantum well is reduced to a one-dimensional problem which, for definiteness, was taken to have the form

$$\left(-\frac{1}{2}\frac{\partial}{\partial z}\frac{1}{m^*(z)}\frac{\partial}{\partial z}+V_{\text{ext}}(z)\right)\Phi_i(z)=\epsilon_i\Phi_i(z), \tag{6}$$

where $V_{\text{ext}}(z)$ is the quantum potential which represents the band-edge changes of the bulk carriers between the two materials of the quantum well structure. Under zero bias conditions, $V_{\text{ext}}(z)$ is constant in each material and its change at the interface is defined in terms of the band offset. $\Phi_i(z)$ is the envelope function of the ith state of a carrier in the quantum well, and $m^*(z)$ is the effective mass (taken as a constant within each material comprising the quantum well). It is worth noting that utilization of Eq. (6) automatically implies a boundary condition of the form

$$\left(\frac{1}{m^*}\frac{d\Phi_i(z)}{dz}\right)\Bigg|_{\text{interface}-\text{CdTe}} =\left(\frac{1}{m^*}\frac{d\Phi_i(z)}{dz}\right)\Bigg|_{\text{interface}-\text{CdMnTe}} \tag{7}$$

i.e., $\Phi(z)$ and $1/m^*\ d\Phi_i(z)/dz$ are continuous at the interface between CdTe and $Cd_{1-x}Mn_xTe$.

Equation (6), under the restraint of the boundary condition (7), is solved by a numerical *shooting* technique. It is to be noted that, in the majority of calculations reported in the literature, the values of the effective masses of the electron, and the light- and heavy- holes used in Eq. (6) are those appropriate to the bulk materials as defined via the bulk band structure. But, in the present work, the value of the effective mass m^* in the (CdTe) well was treated as a parameter which was adjusted for wells of varying width, until the energy levels of the electron, heavy and light holes agreed with those obtain from the pseudopotential calculation. On other hand, the value of m^* for the $Cd_{1-x}Mn_xTe$ was kept at its bulk value since the widths of the barrier layers are much thicker than those of the well layers and could be considered to be ''bulk-like.'' The effective masses appropriate to bulk $Cd_{1-x}Mn_xTe$ were obtained from our recent pseudopotential calculation of the band structure of $Cd_{1-x}Mn_xTe$[25] as a function of the alloy concentration x.

In the class (2) model, the states of the quantum well are expanded in terms of a linear combinations of the periodic parts of the zone center Bloch function appropriate to bulk materials, i.e.,

$$\Phi(\mathbf{r})=e^{i\mathbf{k}_\perp\cdot\mathbf{r}}\sum_{l=1}^{N}u_{l\Gamma}(\mathbf{r})f_l(z), \tag{8}$$

where $\mathbf{k}_\perp$ is the in-plane wave vector, $u_{l\Gamma}(\mathbf{r})$ is the part of the zone center Bloch function with the period of the bulk unit cell, and $f_l(z)$ is the envelope function. At this stage, two assumptions are made: (1) $u_{l\Gamma}(r)$ takes the same form in both well (CdTe) and barrier material ($Cd_{1-x}Mn_xTe$). (2) $f_l(z)$ is slowly varying on the scale of the unit cell appropriate to bulk material.

Substituting Eq. (8) into the Schrödinger equation of the quantum well, and utilizing the property of $u_{l\Gamma}(r)$, we can establish a set of N coupled partial differential equations. In the present work, we use the $\mathbf{k}\cdot\mathbf{p}$ model for the quantum well system developed by Ekenberg *et al.*[40] and emphasis is paid to the hole energy levels. In particular, the Luttinger parameters are directly related to the band−edge effective masses through the relations[41]

$$\frac{m_0}{m^*_{\text{hh}}[100]}=\gamma_1-2\gamma_2, \tag{9a}$$

$$\frac{m_0}{m^*_{\text{lh}}[100]}=\gamma_1+2\gamma_2, \tag{9b}$$

$$\frac{m_0}{m^*_{\text{hh}}[111]}=\gamma_1-2\gamma_3, \tag{9c}$$

$$\frac{m_0}{m^*_{\mathrm{lh}}[111]} = \gamma_1 + 2\gamma_3, \tag{9d}$$

$$\frac{m_0}{m^*_{\mathrm{el}}} = \alpha + \frac{E_p(E_g + \frac{2}{3}\Delta)}{E_g(E_g+\Delta)}, \text{ and} \tag{9e}$$

$$\frac{m_0}{m^*_{s-o}} = \gamma_1 - \frac{E_p\Delta}{3E_g(E_g+\Delta)}, \tag{9f}$$

where γ_1, γ_2, γ_3, α, and E_p are the Luttinger parameters[4] which are shown in Table I. E_g and Δ are band gap and spin-orbit gap, respectively. The m^* are the effective masses along the different directions. It is well known that the Luttinger parameters reflect the effects of microscopic potential in the form of the $V(\mathbf{k})$, and that, in general, they are energy dependent. Consequently, even if the Luttinger formalism could be applied to quantum well structures (a feature which we have shown recently is questionable),[42] the energy dependence of the parametrization scheme would need to be incorporated into the formalism, particularly for narrow wells. This is achieved in the present work by deducing the Luttinger parameters via Eq. (9), utilizing effective masses obtained by fitting the results of Eq. (6), for a given quantum well structure, to the pseudopotential calculation for this same structure.

IV. NUMERICAL RESULTS AND DISCUSSION

A. Comparisons of the single band envelope function model and the pseudopotential calculation

Figures 2(a) and 2(b) plots, respectively, the confinement energies of electron, light-, and heavy-hole ground states as a function of the width of the CdTe quantum well when surrounded by $Cd_{0.9}Mn_{0.1}Te$. Two curves are displayed: (i) PP-full pseudopotential calculation of the electron and hole energy levels in the quantum wells. (ii) EFA-single band envelope function model as summarized by Eq (6). It is clear that the curve given by the EFA model does agree well with that given by the microscopic PP model within quite a large range of the wide wells, i.e., the discrepancy between two sets of the curves is less than 3 meV for the well widths greater than 50 Å. However in all three cases, the discrepancy between the two models increases as the well width decreases. This is attributed to a steady decrease of the applicability of bulk band structure considerations (in the form of the bulk effective mass parameters) to narrow quantum well structures. This is predicated on the reasonable assumption that the pseudopotential, being a microscopic model, gives a more accurate description of narrow wells.

The effective masses which appear in Fig. 3 are deduced by adjusting their values in Eq. (6) until exact agreement is obtained with the PP calculation of the corresponding one electron energy. It is apparent that the expected limit of bulk mass values for the wide wells is obeyed. For CdTe wells of width greater than 50 Å, the effective masses of the electron, light-, and heavy- holes increase by less than 10%, 8%, and 17% of their bulk values, respectively. However, increasingly larger effective masses must be employed in narrower wells in order to eliminate the discrepancy in energies shown in Figs. 2(a) and 2(b). In particular, these effective masses reach values which are double that of the bulk at around 13 Å (4 monolayers). Figure 3 also suggests an empirical relationship between m^* and the well width l_w of the form

$$m^*(l_w) = m' e^{-l_w/L} + m^*_{\mathrm{bulk}}. \tag{10}$$

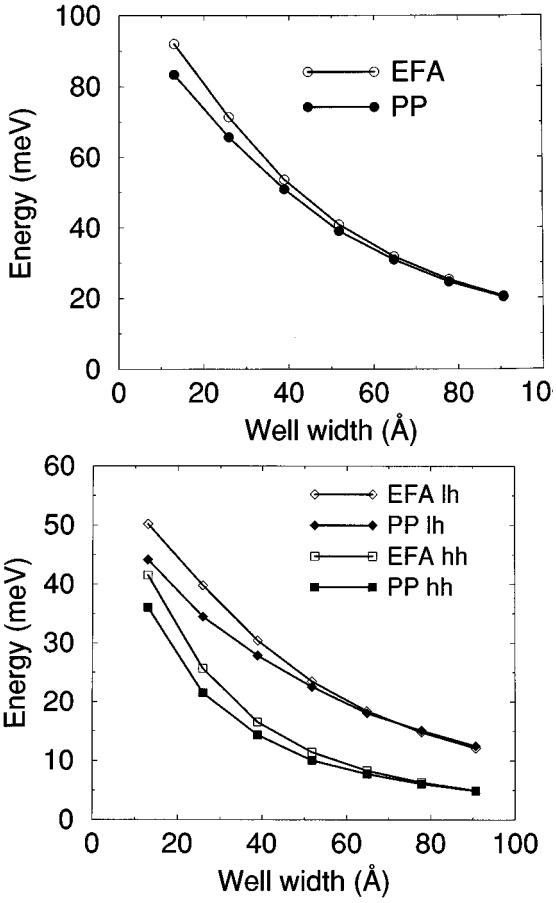

FIG. 2. The dependence of the confinement energies of (a) electron and (b) light- and heavy-holes on the quantum well widths. PP and EFA correspond to the pseudopotential and single-band envelope function models, respectively.

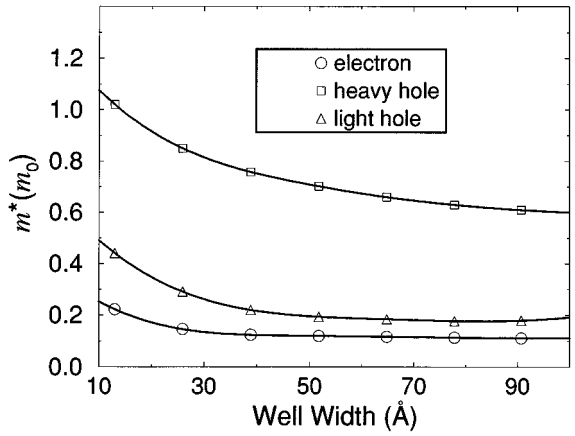

FIG. 3. The dependence of the effective masses of electron, light- and heavy-holes on the quantum well widths.

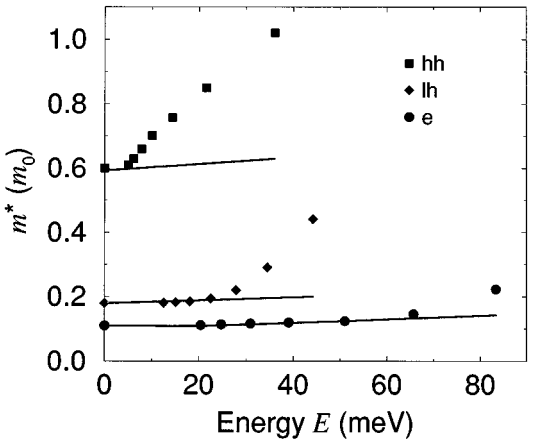

FIG. 4. The effective masses of the electron, light-, and heavy-holes as a function of the confinement energies. The solid points are from the pseudopotential calculations and the solid lines from nonparabolicity approach (see Ref. 42.

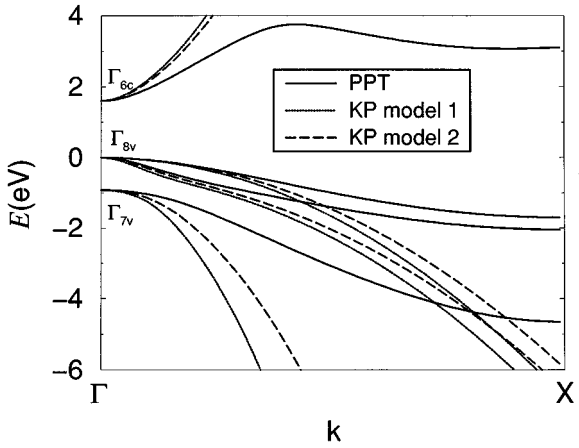

FIG. 5. The band structure of bulk CdTe along (001) calculated with the pseudopotential approach (PP), the $\mathbf{k}\cdot\mathbf{p}$ model with Luttinger parameters deduced from Ref. 42 (KP model 1), and the $\mathbf{k}\cdot\mathbf{p}$ model with Luttinger parameters deduced [via Eq. (9) from the pseudopotential data shown in Table I (KP model 2].

This relationship was fitted to the data in Fig. 3 and gave the values of the constants m' and L as shown in Table III.

It is interesting to note that well width dependent effective masses have been proposed before by Ekenberg,[43] who applied the nonparabolicity correction of bulk band structure to the confinement energy of a subband of a quantum well. In particular, as the quantum well becomes narrower, the wave vector k_z along the growth-axis, which appears in the one-dimensional envelope function $\cos(k_z z)$, becomes larger. The effective mass of the corresponding bulk states can become altered due to the deviation of the bulk band structure from the parabolic $E \propto k^2$ relationship, and hence the effective mass becomes a function of well width. In Fig. 4, the effective mass of Fig. 3 are plotted against the corresponding confinement energies, as illustrated by the solid symbols. In comparison with this, the solid lines are the results of implementing the approach of Ekenberg.[43] Basically this involves deducing the effective mass from the bulk [100] bandstructure[25] at the band energies corresponding to the quantum well confinement energies. It is apparent that while the nonparabolicity of the bulk band structure is contributing to the variation in the effective mass, it is not sufficient to explain the dependency.

B. Comparisons of the multiple-band k·p model and the pseudopotential calculation

Figure 5 displays the band structure of bulk CdTe along (001) calculated with three different methods. The first method employs the pseudopotential approach (PP), the second method the $\mathbf{k}\cdot\mathbf{p}$ model with Luttinger parameters deduced from experimental data of cyclotron resonance[44] (KP model 1), while the third employs the $\mathbf{k}\cdot\mathbf{p}$ model with Luttinger parameters deduced [via Eq. (9) from the pseudopotential data shown in Table I (KP model 2]. It is clear from this figure that both $\mathbf{k}\cdot\mathbf{p}$ models have a dispersion curve which agrees well with that from the pseudopotential approach in a small region near the Γ point. This demonstrates clearly that the $\mathbf{k}\cdot\mathbf{p}$ model is a successful model in the vicinity of a special point of the bulk Brillioun zone. However, beyond that small region, the discrepancy between the $\mathbf{k}\cdot\mathbf{p}$ model and the pseudopotential calculation can be very large (up to several eVs). This has significant implications for the $\mathbf{k}\cdot\mathbf{p}$ model description of a quantum well, particularly a narrow quantum well, where it has been shown[42] that more bulk Bloch functions (i.e., more band states) need to be included in the $\mathbf{k}\cdot\mathbf{p}$ basis set for a quantum well system than are required for the description of a bulk state. Given that the energy levels of these bulk Bloch functions are themselves described poorly by the $\mathbf{k}\cdot\mathbf{p}$ model, it is clear how errors can enter into the $\mathbf{k}\cdot\mathbf{p}$ calculation for a quantum well system. One means of overcoming this would be to increase the number of Luttinger parameters employed.[42] Another approach would be to adopt the energy dependent (i.e., well width dependent) Luttinger parameters.

Figure 6 shows the well width dependence of the Luttinger parameters γ_1 and γ_2 as defined by Eqs. (9a) and Eq. (9b), where the corresponding $m^*_{\mathrm{hh}}[100]$ and $m^*_{\mathrm{lh}}[100]$ come

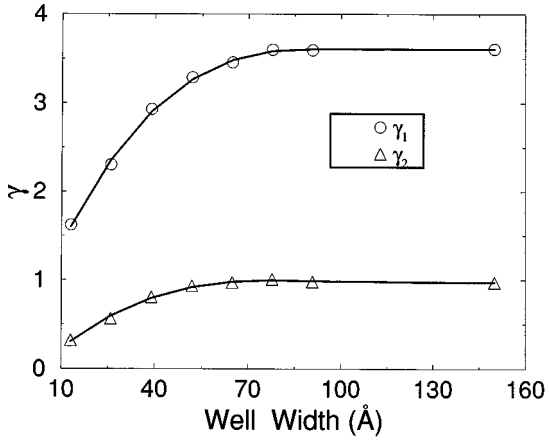

FIG. 6. The dependence of the Luttinger parameters γ_1 and γ_2 on the quantum well widths.

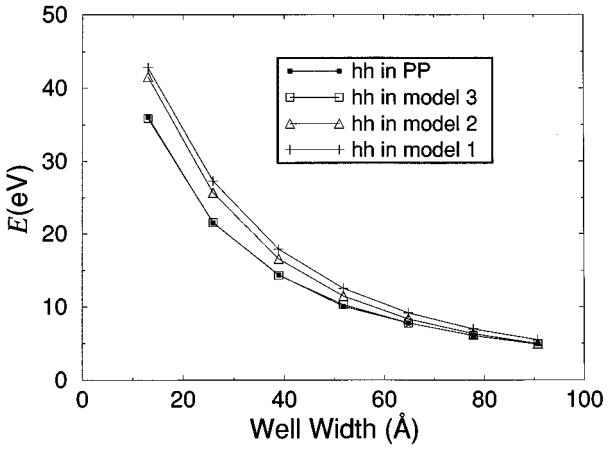

FIG. 7. The heavy-hole confinement energies in the quantum wells calculated with four different approaches.

from Fig. 3 or Eq. (10). When these Luttinger parameters, together with γ_3 appropriate to the bulk value, are put into the calculation, they produce the same confinement energy of the ground heavy- and light- hole states obtained from the pseudopotential calculation shown in Fig. 2(b). The errors are within 0.2 meV. This shows the self-consistency of the calculation even when the masses are taken from a different model. It can be seen from Fig. 6 that the Luttinger parameters corresponding to the narrow wells deviate significantly from their bulk values. This again serves to illustrate the relative crudity of the approximation of using γ_1 and γ_2 values deduced from observation of *bulk* properties.

For completeness, the four curves in Fig. 7 display all the approaches to the heavy-hole energy calculation adopted in the present article. Curve (i) is from PP, a full empirical pseudopotential calculation. Curve (ii) is from the $\mathbf{k}\cdot\mathbf{p}$ model 3, which employs the well width dependent Luttinger parameters given in Fig. 6. Curve (iii) is from the $\mathbf{k}\cdot\mathbf{p}$ model 2, which uses constant Luttinger parameters appropriate to bulk effective masses deduced from the bulk pseudopotential calculations shown in Table I.[25] Curve (iv) is from the $\mathbf{k}\cdot\mathbf{p}$ model 1, which uses constant Luttinger parameters derived from the experimental observations of bulk materials.[44]

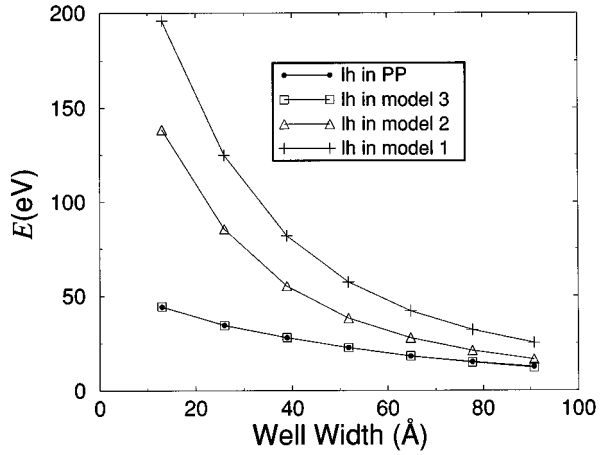

FIG. 8. The light- hole confinement energy in the quantum wells calculated with the same approaches as in Fig. 7.

Figure 8 displays the equivalent data of Fig. 7 but for the light hole. These curves substantiate the point that the utilization of constant (bulk) Luttinger parameters are totally inappropriate for the calculation of the energy level structure of narrow quantum wells.

V. CONCLUSION

It has been demonstrated that calculations of the electron and hole energy levels in narrow quantum wells, based on the envelope function approach employing effective masses, or equivalently Luttinger parameters, deduced from bulk band structure properties, can have large discrepancies compared with the rigorous microscopic approach of the empirical pseudopotential method. Indeed both the effective mass and Luttinger parameters have been shown to have appreciable structural (i.e., well width) dependencies. These dependencies have been illustrated in detail, for the $CdTe/Cd_{1-x}Mn_xTe$ system. As described in more detail in the text, these discrepancies can be regarded as a manifestation of the inappropriateness of the envelope function methods employing structurally independent effective masses within the standard form of the Hamiltonian, which will overestimate considerably the quantum confinement energies in such systems.

[1] S. S. Nedorezov, Sov. Phys. Solid State **12**, 1814 (1971).
[2] G. Barstard, Phys. Rev. B **24**, 5693 (1981).
[3] G. Barstard, Phys. Rev. B **25**, 7584 (1982).
[4] G. Barstard, *Wave Mechanics Applied to Semiconductor Heterostructures* (Les Edition de Physique, Les Ulis, France, 1988).
[5] D. L. Smith and C. Mailhiot, Rev. Mod. Phys. **62**, 173 (1990).
[6] D. L. Smith and C. Mailhiot, Phys. Rev. B **33**, 8345 (1986).
[7] S. Schmitt-Rink, D. S. Chemla, and D. A. B. Miller, Adv. Phys. **38**, 89 (1989).
[8] T. Stirner, P. Harrison, W. E. Hagston, and J. P. Goodwin, Phys. Rev. B **50**, 5713 (1994).
[9] G. Barstard, J. A. Brum, and R. Ferreira, in *Solid State Physics, Advances in Research and Applications*, edited by H. Ehrenreich and D. Turnbull (Academic, New York, 1991), Vol. 44, p. 229.
[10] S. R. Jackson, J. E. Nicholls, W. E. Hagston, P. Harrison, T. Stirner, J. H. C. Hogg, B. Lunn, and D. E. Ashenford, Phys. Rev. B **50**, 5392 (1994).
[11] P. Harrison, F. Long, and W. E. Hagston, Superlattices Microstruct. **19**, 123 (1996).
[12] M. V. Rama Krishna and R. A. Friensner, Phys. Rev. Lett. **67**, 629 (1991).
[13] M. G. Burt, Semicond. Sci. Technol. **3**, 739 (1988).
[14] M. G. Burt, J. Phys.: Condens. Matter **4**, 6651 (1992).
[15] M. G. Burt, Phys. Rev. B **50**, 7518 (1994).
[16] B. A. Foreman, Phys. Rev. B **52**, 12 241 (1995).
[17] P. Vogl, H. P. Hjalmarson, and J. Dow, J. Phys. Chem. Solids **44**, 365 (1983).
[18] M. Jaros, K. B. Wong, and M. A. Gell, Phys. Rev. B **31**, 1205 (1985).
[19] M. A. Gell, D. Ninno, M. Jaros, and D. C. Herbert, Phys. Rev. B **34**, 2416 (1986).
[20] L.-W. Wang and A. Zunger, J. Chem. Phys. **100**, 2394 (1994).
[21] K. Mäder, L.-W. Wang, and Z. Zunger, Phys. Rev. Lett. **74**, 2555 (1995).
[22] K. Mäder, L.-W. Wang, and Z. Zunger, J. Appl. Phys. **78**, 6639 (1995).
[23] L.-W. Wang, A. Zunger, and K. Mäder, Phys. Rev. B **53**, 2010 (1996).
[24] D. M. Wood and A. Zunger, Phys. Rev. B **53**, 7948 (1996).
[25] F. Long, P. Harrison, and W. E. Hagston, J. Appl. Phys. **79**, 6939 (1996).
[26] B. Kuhn-Heinrich, W. Ossau, T. Litz, A. Wang, and G. Landwehr, J. Appl. Phys. **75**, 8046 (1994).
[27] G. Peter, E. Deleporte, J. M. Berroir, C. Delalande, J. M. Hong, and L. L. Chang, Phys. Rev. B **44**, 11 302 (1991).
[28] T. Piorek, W. E. Hagston, and P. Harrison, Phys. Rev. B **52**, 14 111 (1995).

[29] D. R. Yakovlev, *Festkörperprobleme/Advances in Solid State Physics*, edited by U. Rössler (Vieweg, Braunschweig, 1992), Vol. 32.
[30] S. Jackson, W. E. Hagston, P. Harrison, J. H. C. Hogg, J. E. Nicholls, B. Lunn, P. Devine, and S. Ali, Phys. Rev. B **49**, 13 512 (1994).
[31] M. Jaros, A. Zoryk, and D. Ninno, Phys. Rev. B **35**, 8277 (1987).
[32] F. Long, S. H. Liu, F. Mei, J. Miao, and J. Liang, Chin. Phys. Lett. **11**, 109 (1994).
[33] M. L. Cohen and T. K. Bergstresser, Phys. Rev. **141**, 789 (1966).
[34] S. Bloom and T. K. Bergstresser, Solid State Commun. **6**, 465 (1968).
[35] P. Harrison, T. Stirner, S. J. Weston, S. R. Bardorf, S. Jackson, W. E. Hagston, J. H. C. Hogg, J. E. Nicholls, and M. O'Neill, Phys. Rev. B **51**, 5477 (1995).
[36] P. Chen, J. E. Nicholls, J. H. C. Hogg, T. Stirner, and W. E. Hagston, Phys. Rev. B **52**, 4732 (1995).
[37] J.-B. Xia, Phys. Rev. B **38**, 8358 (1988).
[38] K. Mäder and A. Zunger, Phys. Rev. B **50**, 17 393 (1994).
[39] A. Blacha, H. Presting, and M. Cardona, Phys. Status Solidi B **126**, 11 (1984).
[40] U. EkenBerg and M. Altarelli, Phys. Rev. B **35**, 7585 (1987).
[41] D. Gershoni, C. H. Henry, and D. A. Baraff, IEEE J. Quantum Electron. **29**, 2433 (1993).
[42] W. E. Hagston and F. Long (unpublished).
[43] U. EkenBerg, Phys. Rev. B **40**, 7714 (1989).
[44] Le Si Dang, G. Neu, and R. Romestain, Solid State Commun. **6**, 1187 (1982).
[45] J. R. Chelikowsky and M. L. Cohen, Phys. Rev. B **14**, 556 (1988).
[46] Ch. Neumann, A. Nöthe, and N. O. Lipari, Phys. Rev. B **37**, 922 (1976).
[47] J. Van Vechten, in *Handbook of Semiconductors*, edited by S. P. Keller (North-Holland, Amsterdam, 1980), Vol. 3, p. 44 .
[48] A. Twadoski, M. Nawrochi, and J. Ginter, Phys. Status Solidi B **96**, 497 (1979).